Domain of Stability Characterization for Power Systems: A Novel Individual Invariance Method

Surour Alaraifi, Seddik Djouadi, *Senior Member, IEEE*, and Mohamed Shawky El Moursi, *Senior Member, IEEE*

***Abstract*—In this article, we approach the problem of stability in nonlinear systems through a new perspective that views them as a combination of individual artificial systems carefully chosen to simplify the complex structure of nonlinear systems. This is achieved by recasting nonlinear vector fields as an algebraic sum of individual vector fields for which artificial systems with known invariant sets or at least in forms that allow for tractable approximation of their invariant sets. This attempt to restructure nonlinear systems stands out in comparison to other previous attempts like Lure' systems or network based models as a purely mathematical structuring technique that transcends the physical constraints and dependencies within dynamical models and allows the user to creatively construct artificial systems with the sole focus on the overall stability. The theoretical foundation is provided for a theorem about individual invariance to relate the invariant sets of individual artificial systems to the invariant set of their original system in a way that significantly simplifies the task of approximating regions of attraction. Several examples are used to demonstrate this theorem and we also evaluate the use this theorem for the challenging power system stability problems in both AC and DC grids. The proposed method is successfully applied to the IEEE 39-bus New England system, and a DC converter with constant power load giving accurate and realistic estimations of the critical clearing time and stability regions in comparison to state of the art approaches.**

***Index Terms*—Critical clearing time, DC microgrid, multi-machine system, stability regions.**

I. Introduction

STABILITY in nonlinear systems has been a central topic of interest for researchers and scientists in almost every field of science and engineering due to the prevailing role of nonlinearities in both nature and industries. Ever since Lyapunov theory was developed, it played a key role in most of the developments in stability theory afterwards. The importance of Lyapunov theory is not limited to its ability to directly certify stability of an equilibrium point but extends also to determining stability regions or regions of attraction [1]. One of the first challenges in Lyapunov stability was and still is to characterize a general form of Lyapunov functions for specific vector fields. Hence, many efforts led to the development of somehow general functions for certain types of vector fields [2], [3].

A Lure' system is a control system described as a linear system with a sector bounded nonlinearity which allows the use of pre-defined nonlinear Lyapunov functions [2], [4]. The importance of Lure's systems became more apparent recently with the developments in Semi Definite Programming (SDP) solvers that allow for efficient solutions of linear matrix inequalities (LMI) appearing naturally in Lure'-type systems [4], [5], [6]. Thus, Lure'-systems remain a topic of interest for researcher in stability analysis and have seen some applications in power systems despite its conservative nature [2], [7]. The literature of stability has also seen attempts to re-define Lyapunov functions. In [8], it was shown that Lyapunov conditions can be relaxed and a Lyapunov function may increase in some subsets as long as it eventually decreases to zero. This relaxation although very helpful and essentially needed, requires extra conditions on higher order derivatives which can limit its applicability to special cases. Other variations of Lyapunov functions were proposed as well. In [9], the notion of vector Lyapunov functions was introduced where instead of searching for a single function, the search is extended to a set of functions giving it more flexibility, however, such results are of practical interest for control design frameworks rather than stability regions' estimation [10], [11], [12]. There are also other methods to Lyapunov functions such as the Zubov's method which can determine the exact region of attraction. Zubov's method is unfortunately theoretical as it requires the solution of a partial differential equation which does not in general has a closed form solution [13].

In power systems which represent one of the most advanced and active application fields of nonlinear systems' stability analysis [14], energy function based approaches dominated stability assessment [15]. These approaches rely on the ability to find an appropriate candidate function and on the computation of the critical energy value at the so-called Controlling Unstable Equilibrium Point (CUEP) with respect to the pre-defined energy function. This task is involving and difficult and can lead to inaccurate stability assessments if the algorithm deviates slightly from the target point. It is true however that among energy function methods, Controlling UEP-based methods can provide less

Manuscript received 12 November 2021; revised 5 March 2022, 7 July 2022, 3 October 2022, and 3 February 2023; accepted 10 February 2023. Date of publication 22 February 2023; date of current version 26 December 2023. This work was supported by Khalifa University under Award CIRA-2018-37. This research work was conducted at Khalifa University. Paper no. TPWRS-01735-2021. *(Corresponding author: Mohamed Shawky El Moursi.)*

Surour Alaraifi and Mohamed Shawky El Moursi are with the Advanced Power and Energy Centre (APEC), EECS Department, Khalifa University of Science and Technology, Abu Dhabi 307501, UAE (e-mail: s.alaraifi@hotmail.com; mohamed.elmoursi@ku.ac.ae).

Seddik Djouadi is with the Department of Electrical Engineering and Computer Science, University of Tennessee, Knoxville, TN 37996-2250 USA (e-mail: mdjouadi@utk.edu).

Color versions of one or more figures in this article are available at https://doi.org/10.1109/TPWRS.2023.3247439.

Digital Object Identifier 10.1109/TPWRS.2023.3247439

conservative estimates. The current accepted method for finding the controlling UEP is called the Boundary of stability region based Controlling UEP method (BCU method) and was proven to have a high success rate [14], [16]. Nevertheless, the BCU method in power systems is not designed to estimate regions of attraction, instead it is designed to estimate the relative boundary of stability region with respect to a fault-on system [16]. Recent results in power system stability focused on Lyapunov functions instead but with no significant computational advantages [7], [17], [18]. In [7], the Popov criterion was used and an optimization problem was formulated to enlarge the region of attraction, however, the results indicate some conservativeness and the dependence on sector bounds further limits its applicability. In [17], [18], Sum Of Squares (SOS) programming techniques were used to estimate the domain of attraction for a simple power system case study but the results did not show a sizable computational advantage.

The move toward renewable generation and the integration of more converter-based devices in the power grids around the world has driven the research on power system stability in recent years away from the classical power system models. In [19], synchronization stability is studied for a Voltage Source Converter (VSC) connected to a grid where a Lyapunov function is constructed through SOS programming and consequently a region of attraction can be approximated with some degree of conservatism. Similarly, Lyapunov based approaches were applied in [20] to characterize the stability boundary of a VSC-grid system using an analytically derived Lyapunov function, whereas, [21] used an SOS program to find a numerical Lyapunov function. Another interesting subject in power system stability is the stability regions of DC systems with Constant Power Loads. In [22], the impact of Constant Power Loads (CPL) in multiconverter automotive power systems was studied and the region of attraction was approximated for a DC converter with CPL by examining the system trajectories near predefined boundary curves. Whereas, in [23], a DC converter with CPL is modeled as a Power-Controlled Hamiltonian and the region of attraction was derived by a quadratic Hamiltonian.

As can be noticed from the literature, stability assessment methods in power systems remain limited to Lyapunov Theorems and the Energy function approach with no notable exception in recent years. This article proposes a novel method to estimate regions of attraction of autonomous nonlinear systems by overlooking the ordinary representation of vector fields and instead reproduce a nonlinear vector field as the algebraic sum of vector fields for which we can develop individual artificial systems with known or at least tractable regions of attraction. In [24], we proposed a similar representation of vector fields and introduced the idea of artificial systems to prove that a Lyapunov function can be constructed from artificial systems independently without the need of considering conditions on the original vector field. In this work, with the help of a newly developed theory we are able to reconstruct the region of attraction of a given system from the individual regions of attraction of the artificial systems without the need of constructing individual functions as in [24]. The results of this article are considered an improvement over our previous results [24] in terms of generality and applicability. Such an approach allows for fast estimation of stability regions and provides an insight on the mathematical interaction of individual vector fields. The proposed concept sets itself apart from the traditional Lyapunov-based methods in its ability to identify each element of a given vector field as an object to enlarge, shrink or deform the stability region in the system under study regardless of the type of the dynamic interaction or dimensionality and proves to be generic enough to address challenging problems like power system transient stability and stability regions in DC circuits.

II. Theoretical Background

Consider an autonomous dynamical system represented by the following differential equation:

$$\dot{x} = f(x), \quad x \in \Re^n \tag{1}$$

The solution starting from x at $t = 0$ is called the trajectory and is denoted by $\varphi(t, x)$. $f(x) : D \to \Re^n$ is a vector valued function from a domain $D \subset \Re^n$ to $\Re^n$ that is referred to as the vector field associated with the state vector x. It is natural to assume that $f(.)$ satisfies sufficient conditions for the existence and uniqueness of solutions. Thus, all required derivatives exist and are continuous. x_e is an equilibrium point if $f(x_e) = 0$. An equilibrium point can be either isolated with no other equilibrium point in its vicinity or can be part of a continuum of equilibrium points (e.g., equilibrium subspace). For the system in (1), assuming without loss of generality that $x_e = 0$, the region of attraction A of the origin is defined as follows:

$$A = \left\{ x \in D : \lim_{t \to \infty} \varphi(t, x) = 0 \right\} \tag{2}$$

The goal is to achieve the largest possible estimate of A. From its definition, A is an invariant set, hence, any trajectory starting in A will remain in it at all time. Generally, the region of attraction is an open, connected and invariant set [1]. These properties are generic and do not serve the development of region of attraction estimation algorithms. A very common approach to satisfying these properties is by finding sub-level sets of Lyapunov functions. For a system defined by (1), the region of attraction of the origin can be estimated by sub-level sets of Lyapunov functions [1]:

$$A_c = \{x \in D : V(x) \leq c\}$$

where $V(x)$ is a Lyapunov function, $c > 0$ and $x_e \in A_c$. Enlarging such approximation have been the target of extensive research in nonlinear systems. It can be seen however, that the problem of estimating the region of attraction by means of Lyapunov functions is twofold. First, finding the appropriate Lyapunov function, and secondly enlarging the estimated region A_c. Lyapunov theory only requires the knowledge of the vector field $f(x)$ and proceeds without any explicit knowledge of solutions, hence, current methods of finding such functions rely on searching for $V(x)$ once the vector field is fixed. In this article, the vector field $f(x)$ is manipulated to re-write it as a sum of vector fields such that each individual vector field is used to construct an artificial system.

III. Individual Invariance

In practice, once a dynamical system is modelled, its model remains intact as long as it passes a certain validation process. This physics inspired practice seems prudent and it definitely is since the vector field in (1) is designed as a mathematical interpretation of physical interactions and only careful breakdown of (1) will result in a physically meaningful vector elements.

In this work, we will try to temporarily untie this physical-mathematical bond and deal with $f(x)$ as a vector field arising from simple algebraic relations between different vectors and elements regardless of their underlying physical interpretation. To be more precise, we will convert the nonlinear dynamical system from the form in (1) to the following form:

$$\dot{x} = \sum_{i=1}^{m} f^i(x) = f(x), \quad x \in \Re^n \tag{3}$$

In (3), clearly if $m = 1$ then we will arrive at the same definition in (1). However, the proposed representation proved to simplify estimating the region of attraction among other advantages as will be discussed hereafter. In the rest of the paper, $\sum_{i=1}^{m} f^i(x)$ and $f(x)$ will be used interchangeably.

Note that every $f^i(x)$ in (3) is an n-dimensional vector that results from any combination of row elements of $f(x)$ and it is fairly simple to reconstruct vectors $f^i(x)$ from any given vector $f(x)$, but the choice of $f^i(x)$'s is crucial in estimating stability regions. We can use each vector field in $\sum_{i=1}^{m} f^i(x)$ to construct artificial dynamical systems each defined as $\dot{x}^i = f^i(x^i)$, where $x^i \in \Re^n$. This anatomy of $f(x)$ evokes an immediate question; what is the relation between the stability region of an artificial system and the stability region of the original system (1)? Apparently, classical linearization approach can tell us that if each linearized artificial system has an asymptotically stable equilibrium point at the origin, then the linearized original system will definitely maintain that property of the origin by superposition. Nevertheless, we can deduce more than that by carefully constructing and examining individual artificial systems and provide a broader answer to the former question.

By dealing with the standard representation of dynamical systems in (1), our focus when studying stability is the vectors orientation of $f(x)$ and their directions in the proximity of equilibrium points (for hyperbolic equilibrium points), whereas, the proposed representation in (3) allows us to choose each $f^i(x)$ as long as the sum of all individual vector fields yields $f(x)$ which to some extent converts the problem from analyzing a given dynamical system to finding proper individual vector fields, hence, a system's stability will be the result of the interaction between its individual vector fields. As seen later, this change in perspective, though straightforward, can tremendously improve our understanding of stability regions. In [24], we illustrated the effectiveness of this representation by developing a new theory that gives rise to a computationally efficient algorithm to estimate stability regions. In this article we provide a generalization to our previous work that overcomes convexity requirement and solves the problem of stability in a novel and distinctive way. Theorem 1 lays the foundation for estimating stability regions of systems in (3) by defining a positively invariant set for a given dynamical system (3) as a region in space where each artificial dynamical system, $\dot{x}^i = f^i(x^i)$, is positively invariant.

Definition 1: For a system defined by (1), we call $A \subset D$ invariant with respect to the flow of (1) if $\varphi(t, x) \in A$ for all $x \in A$ and all $t \in \Re$. We also call A positively invariant if $\varphi(t, x) \in A$ for all $x \in A$ and all $t \geq 0$.

Theorem 1: For a system defined by (3), define $\dot{x}^i = f^i(x^i)$, with $f^i(x^i) : D \to \Re^n, \forall i \in [1, m]$ and let $D \subset \Re^n$ be a neighborhood of $\omega_i, \forall i \in [1, m]$. If there exists a set $A_e \subset D$ with $A_e = \{x \in D : \lim_{t\to\infty} \varphi^i(t, x) = \omega_i, \forall i \in [1, m]\}$, where $\varphi^i(t, x)$ is a solution of each system $\dot{x}^i = f^i(x^i)$ starting at x, then A_e is positively invariant under the flow of the original system (3).

Proof: To prove that A_e is positively invariant with respect to (3), it is necessary to show that $\sum_{i=1}^{m} f^i(x)$ is an "inward" pointing vector along the boundary of A_e denoted as ∂A_e. From the theorem statement, it is given that A_e is positively invariant under the flow of each artificial system given by:

$$\dot{x}^i = f^i(x^i) \tag{4}$$

Hence a trajectory $\varphi^i(t, x)$ initiated at any $x \in A_e$ lies entirely in A_e for $t \geq 0$ so we can say that $f^i(x)$ points "inward" along ∂A_e for all $i \in [1, m]$ due to individual invariance [25]. This is equivalent to:

$$\left\langle f^i(x), x - y \right\rangle \geq 0$$

For any point $x \in A_e$ and $y \in \Re^n$ with $\|x - y\| = dist(y, A_e)$ and for all $i \in [1, m]$. $dist(y, A_e)$ denotes the (shortest) distance from y to A_e, which is always attained since A_e is a closed set, and $< \cdot, \cdot >$ denotes the Euclidean inner product. By summing over i we get:

$$\sum_{i=1}^{m} \left\langle f^i(x), x - y \right\rangle = \left\langle f(x), x - y \right\rangle \geq 0$$

This confirms the orientation of $f(x)$ toward the interior of A_e for any point x belongs to the boundary of A_e so no trajectory of (3) can escape A_e for $t \geq 0$ and this proves its positive invariance under the flow of (3). ■

Note that if A_e has a smooth boundary, we could follow an argument similar to Bony-Brezis theorem [26], [27], with $v(x)$ as an exterior normal vector at a point x in ∂A_e, then we will have $\left\langle f^i(x), v(x) \right\rangle \leq 0$ which is true for all $i \in [1, m]$ due to the individual invariance condition in the theorem and eventually by summing over i we can arrive at the inequality $\left\langle f(x), v(x) \right\rangle \leq 0$ which holds true for any point at ∂A_e. The geometrical interpretation of non-smooth and smooth boundaries of ∂A_e are provided in Figs. 1 and 2 respectively.

Corollary 1: For a system defined by (3), if there exists $\dot{x}^i = f^i(x^i), \forall i \in [1, m]$ with $A_i = \{x \in D : \lim_{t\to\infty} \varphi^i(t, x) = \omega_i, f^i(\omega_i) = 0\}, \forall i \in [1, m]$, then $A_e = \bigcap_{i\in[1,m]} A_i$ is positively invariant with respect to the original system (3) if $\omega_i \subset A_e, \forall i \in [1, m]$.

The proof of this corollary follows immediately from Theorem 1 but the importance of this corollary is that it provides a practical guideline to defining A_e with respect to individual systems. Theorem 1 identifies invariant sets of an autonomous

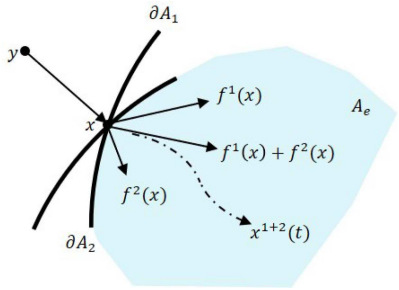

Fig. 1. Geometrical interpretation of Theorem 1 proof.

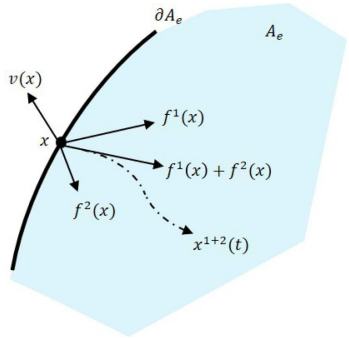

Fig. 2. Geometrical interpretation of Theorem 1 proof for smooth ∂A_e.

dynamical system by examining the individual vector fields $f^i(x)$ that constitute $f(x)$. Generally, finding an invariant set for a given vector field is not an easy task, however, Theorem 1 does not constraint the choice of individual vectors to a certain form which allows in many cases the construction of simplified individual vector fields with analytically defined invariant sets as will be illustrated in the next section. But before proceeding, there are several important remarks about Theorem 1:

Remark 1: Each artificial system can have a different attraction set ω_i which could be an equilibrium point, a continuum of equilibrium points, a limit cycle, or even multiple limit sets.

Remark 2: The existence of A_e does not rule out the possibility of having strange attractors or periodic solutions within A_e.

Remark 3: If A_e is a compact set, then the ω-limit set is not empty. This remark is of practical importance since it qualifies A_e as a region of attraction when the only ω-limit is an attractor.

The remarks are critical for understanding individual invariance as they set it apart from standard Lyapunov theory or Energy function concepts and give an insight into the level of generality of this concept. For instance, Remarks 1 and 2 indicate that a set A_e in Theorem 1 is not necessarily defined for equilibrium points but also can contain limit cycles or multiple limit sets and can in theory contain a strange attractor. In contrast, the existence of Lyapunov function rules out the possibility of limit cycles within its domain. In terms of applying Theorem 1 and its corollary, the conditions of Remark 3 are sufficient for sets obtained by Theorem 1 to qualify as stability regions and this remark will be used throughout this article. The following test systems will clarify how Thoerem 1 and its corollary can be used to provide an estimate of region of attraction for autonomous dynamical systems.

IV. Numerical Results

In this section, we will illustrate the application of the theorem of individual invariance and the flexibility produced from transforming system (1) to (3).

I) Consider the second order system that represents a reduced order two machines system given by [14], [16]:

$$\begin{aligned}\dot{x}_1 &= -a_1 \sin x_1 - b \sin(x_1 - x_2)\\ \dot{x}_2 &= -a_2 \sin x_2 - b \sin(x_2 - x_1)\end{aligned} \tag{5}$$

where a_1, a_2 and b are positive real numbers. Let us define three individual artificial systems as follows:

$$\begin{bmatrix}\dot{x}_1 = -a_1 \sin x_1\\ \dot{x}_2 = 0\end{bmatrix}, \begin{bmatrix}\dot{x}_1 = 0\\ \dot{x}_2 = -a_2 \sin x_2\end{bmatrix}, \begin{bmatrix}\dot{x}_1 = -b \sin(x_1 - x_2)\\ \dot{x}_2 = -b \sin(x_2 - x_1)\end{bmatrix}$$

Corollary 1 can be applied now by identifying individual invariance sets ω_i for each artificial system $\dot{x}^i = f^i(x^i)$ as follows:

$$\begin{aligned}A_1 &= \{x \in \Re^2 : |x_1| \le \pi\},\\ A_2 &= \{x \in \Re^2 : |x_2| \le \pi\},\\ A_3 &= \{x \in \Re^2 : |x_1 - x_2| \le \pi\}\end{aligned} \tag{6}$$

The artificial systems 1 and 2 refer to machines 1 and 2 respectively while $f^3(x)$ represents a coupled nonlinear interaction with a stable equilibrium subspace $\{x \in \Re^2 : x_1 - x_2 = 0\}$ and unstable equilibrium subspaces at $\{x \in \Re^2 : x_1 - x_2 = -\pi\}$ and $\{x \in \Re^2 : x_1 - x_2 = \pi\}$. Thus, the polyhedron defined by A_3 is an invariant set and the intersection of sets in (6) yields the following invariant set:

$$A_e = \{x \in \Re^n : \|x\|_\infty \le \pi, |x_1 - x_2| \le \pi\}$$

From remark 2, A_e is a region of attraction for the origin. Fig. 3 illustrates the estimated region of attraction and compares it to the largest compact set A_V of an energy function of (5) as given in [28]. Not only that individual invariance approach compares favorably in terms of estimated size but also in the ability to arrive at an analytically defined set unlike A_V which requires finding the closest unstable equilibrium point, defining an energy function, and using the level set of the energy function at the closest unstable equilibrium point as the stability region boundary which is only valid if the level set is compact.

II) Consider the following second order system that shares similar nonlinearities as the reduced order flux decay model given by [15]:

$$\begin{aligned}\dot{x}_1 &= -a x_2 \sin x_1\\ \dot{x}_2 &= -b x_2 + c \cos x_1\end{aligned} \tag{7}$$

where a, b and c are positive real numbers. Let us define two individual artificial systems as follows:

$$\begin{bmatrix}\dot{x}_1 = -a x_2 \sin x_1\\ \dot{x}_2 = 0\end{bmatrix}, \begin{bmatrix}\dot{x}_1 = 0\\ \dot{x}_2 = -b x_2 + c \cos x_1\end{bmatrix}$$

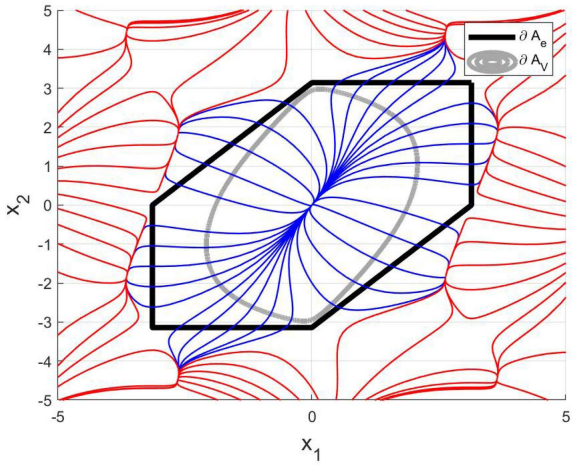

Fig. 3. Vector field of (5) with $a_1 = 1, a_2 = 0.5, b = 0.5$.

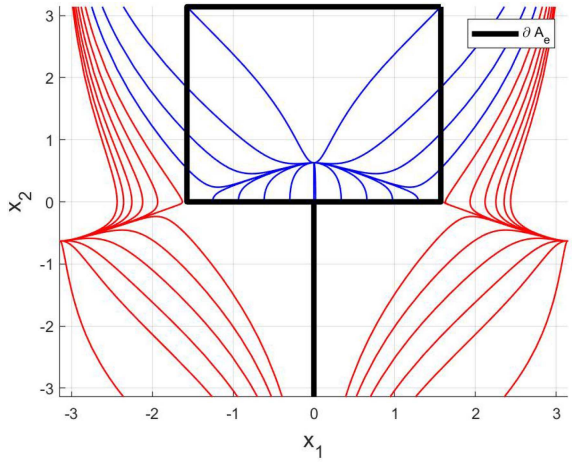

Fig. 4. Vector field of (7) with $a = 2, b = 2.7, c = 1.7$.

Similar to example I, Corollary 1 can be applied now by identifying invariant sets A_i for each artificial system $\dot{x}^i = f^i(x^i)$ as follows:

$$A_1 = \left\{x \in \Re^2 : |x_1| \leq \pi, x_2 \geq 0\right\},$$
$$A_2 = \left\{x \in \Re^2 : |x_1| \leq \frac{\pi}{2}\right\}, \tag{8}$$

By inspection, the artificial system 1 requires the nonnegativity of x_2 in order to maintain the negativity of the quantity $-ax_2 \sin x_1$ and it also requires x_1 to be in the set $\{x_1 : |x_1| \leq \pi\}$ which guarantees that trajectories of the artificial system will converge to the continuum of stable equilibrium points defined as $\{x \in \Re^2 : x_1 = 0, x_2 \geq 0\}$. $f^2(x)$ represents a more complicated behavior, with continuum of stable equilibrium points defined as $\{x \in \Re^2 : x_2 = \frac{c}{b} \cos x_1\}$. However, since artificial system 1 restricts x_2 to be nonnegative, then, it is easy to see that x_1 lies in the set A_2 as defined above. By applying Theorem 1, the intersection of sets in (8) yields the following invariant set:

$$A_e = \left\{x \in \Re^n : |x_1| \leq \frac{\pi}{2}, x_2 \geq 0\right\}$$

The equilibrium point in A_e is $x_e = \{0, \frac{c}{b}\}$ and is unique and asymptotically stable. Fig. 4 illustrates the estimated region of attraction as well as the polytope A_e.

III) The previous examples dealt with convex estimations of stability regions. In this example we demonstrate the possibility of defining non-convex sets as regions of attraction by applying individual invariance. Consider the second order system given by [29]:

$$\dot{x}_1 = -x_1 + 2x_1^2 x_2$$
$$\dot{x}_2 = -x_2 \tag{9}$$

Let us define the individual artificial systems as follows:

$$\dot{x}_1 = -x_1 + 2{x_1}^2 x_2 \qquad \dot{x}_1 = 0$$
$$\dot{x}_2 = 0 \quad , \qquad \dot{x}_2 = -x_2$$

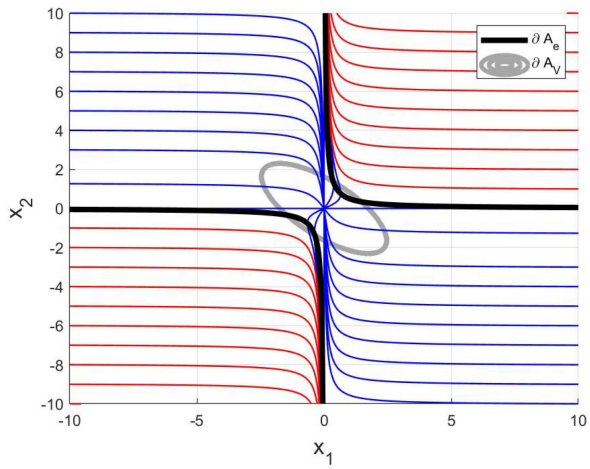

Fig. 5. Phase portrait of Example 3 (9).

Corollary 1 can be applied now by identifying invariant sets A_i for each artificial system $\dot{x}^i = f^i(x^i)$ as follows:

$$A_1 = \left\{x \in \Re^2 : |x_2| \leq \frac{1}{2x_1}\right\},$$
$$A_2 = \{x \in \Re^2\}, \tag{10}$$

Analytically, artificial system 1 has an equilibrium set at $(0, x_2)$ and at $(x_1, \frac{1}{2x_1})$ with former being the stable set and the latter is an unstable set. Since the second artificial system is globally stable at $(x_1, 0)$, we can use the intersection of A_1 and A_2 as our estimate for A_e.

By applying Corollary 1, the intersection of sets in (10) yields the following invariant set:

$$A_e = A_1 = \left\{x \in \Re^n : |x_2| \leq \frac{1}{2x_1}\right\}$$

The equilibrium point inside A_e is at the origin, unique and asymptotically stable. Fig. 5 illustrates the estimated region of attraction A_e and compares it to an optimal estimation from Lyapunov function in [29]. This result is of significant importance

considering that most estimation approaches rely on solving convex problems and end up with convex estimates that are naturally very conservative [7], [17].

Individual invariance theorem requires restructuring the system under study by defining artificial systems but it does not define or constrain the choice of artificial systems since no general way can possibly exist to choose individual vector fields for any nonlinear system and that will always be system dependent. This seemingly intuitive limitation is reminiscent of a Lyaponuv theory shortcoming where finding a Lyapunov function remains a system dependent attribute. However, as seen in the previous examples and as will be seen in the next sections, choosing individual vector fields can be done analytically with no computational cost and can be straightforward in many applications.

It is worth mentioning that, choosing an artificial system that contains the stable equilibrium point of the original system at its limit can provide significant ease in many cases. Also, in other cases, it is useful to isolate the linear and nonlinear parts of a system into different artificial systems. One useful approach that is possible with artificial systems is to introduce an auxiliary vector field to help in moving the limit set of artificial systems as described in Section VI.

In the next sections, two different stability problems will be studied to illustrate the superiority of individual invariance in power systems and power electronics applications. The first application is for AC power systems, the well-known transient stability problem where the largest fault clearing time is defined as the longest fault duration a system could withstand while maintaining synchronism and is called the Critical Clearing Time (CCT) [30]. Larger estimates of stability regions means that fault-on trajectory could stay longer on that region before the system is considered unstable. The other application is stability region estimation for a DC converter with a Constant Power Load (CPL) where its stability is usually studied using linear analysis [22]. The two applications have different objectives, in the former the goal is to make sure that fault clearing times are within CCT values, whereas in the latter, the goal is to design the proper parameters of the converter. In both cases, individual invariance is proven to provide accurate and reliable estimates in comparison to standard and state of the art methods in the literature.

V. Transient Stability

For the purpose of this article we will consider a classical power system of n synchronous generators with each generator's dynamics represented by the swing equation and all generators are modeled as constant voltage behind reactance. By assuming fixed impedance loads, the power system model is governed by the following set of nonlinear differential equations [16]:

$$\begin{aligned}\dot{\delta}_i &= \omega_i \\ M_i\dot{\omega}_i &= P_i - \sum_{j=1}^{n}(V_iV_jB_{ij}\sin(\delta_{ij})) - D_i\omega_i \end{aligned} \tag{11}$$

Where the subscript i represents the machine number, M_i, D_i are the inertia constant and damping coefficient for the i_{th} machine, respectively, P_i is the mechanical power input, V_i is the i_{th} generator's bus voltage magnitude and B_{ij} represents the line admittance. The model describes the dynamics of two states: δ_i, the generator's angle and ω_i the generator's angular speed. This model is known as the classical power system model and have been used extensively in the power system stability literature. Although this model is considered as a simplified model, assessing stability for such model was proven to be a difficult task [31].

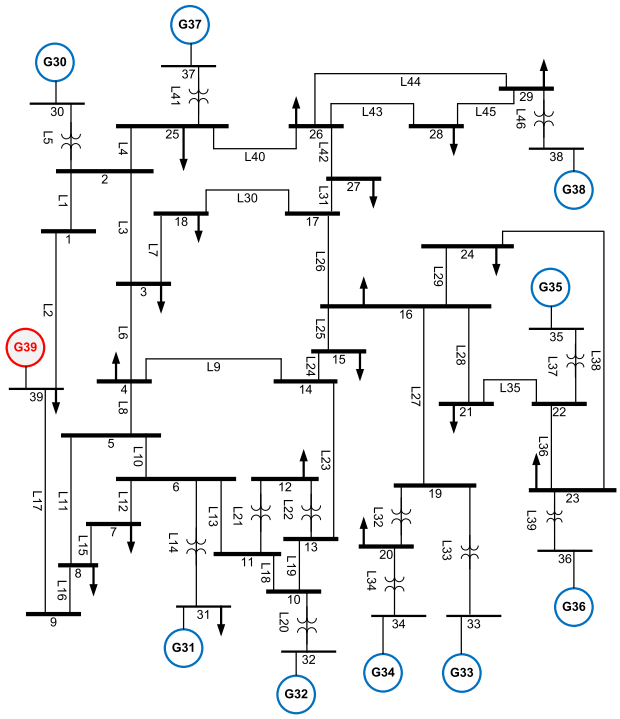

Fig. 6. The 39-bus system.

A. New England 39-Bus System (Associated Gradient System)

The New England 10-machines 39-bus system is a network reduced model representing a reduced model of the transmission network in New England [15]. As depicted in Fig. 6, the system can be further reduced by reconstructing the Admittance matrix retaining only machines' buses in a common procedure as given in [15], [28].

By taking machine 1 as reference and introducing new variables $\delta_{i,1} = \delta_i - \delta_1, \forall i = [2, n]$, the electric power in (11) can be expressed in terms of the new variables as follows:

$$P_{e,i}(\delta_{2,1}, \ldots, \delta_{n,1}) = \sum_{j=1, j\neq i}^{n} V_iV_jB_{ij}\sin(\delta_{i,1} - \delta_{j,1})$$

That leads to the following modification to model (11):

$$\begin{aligned}\dot{\delta}_{j,1} &= \omega_j - \omega_1 && \forall j = [2, n] \\ M_i\dot{\omega}_i &= P_i - P_{e,i}(\delta_{2,1}, \ldots, \delta_{n,1}) - D_i\omega_i && \forall i = [1, n]\end{aligned} \tag{12}$$

Algorithm 1: Algorithm for Finding the Critical Clearing Time Given A Candidate $\mathcal{P}$ and $\{x^f(t)\}$.

1 Start
  Input : $\mathcal{P}$, $x^f(t)$, Δt, and t_{max}
  Output: t_c
2 **if** $\exists x : \mathcal{P}(x) \neq \emptyset$ **then**
3 | go to 7
4 **else**
5 | go to 11
6 **end**
7 $t = 0$;
8 **while** $\{x^f(t)\} \bigcap \mathcal{P} \neq \emptyset$ **or** $t \leq t_{max}$
9 $t = t + \Delta t$
10 $t_c = t$
11 **end**

Which gives the following reduced order model [16]:

$$\dot{\delta}_{j,1} = P_j - P_{e,j}(\delta_{j,1}, \ldots, \delta_{n,1}) \quad \forall j = [2, n] \tag{13}$$

The reduced order model (13) represents the associated gradient model of (12) and will be used to estimate the critical clearing time using the individual invariance theorem in multi-machine power systems. Note that a multi-machine power system in this form has an energy function defined as [28]:

$$E(x) = -\sum_{i=2}^{n} P_i(\delta_{i,1} - \delta^*_{i,1}) - \sum_{i=2}^{n}\sum_{j=1, j\neq i}^{n} V_i V_j B_{ij}\{cos(\delta_{i,1} - \delta_{j,1}) - cos(\delta^*_{i,1} - \delta^*_{j,1})\} \tag{14}$$

For the required simulations, bus 1 is considered as a slack bus (see Appendix A) which puts the system in the form given in (13). Each $\delta_{i,j}$ in (13) will be invariant in the set $A_i = \{\delta_{i,j} \in \Re^n : |\delta_{i,j} - \delta^*_{i,j}| \leq \pi, \forall i, j \in [1, n]\}$ with $\delta^*_{i,j}$ being the fixed point of (13).

With every A_i representing a polyhedron, the region of attraction for (13) is estimated as the intersection of polyhedrons that can be described as:

$$\mathcal{P} = \{x \in \Re^n : \mathcal{A}x \leq b\} \tag{15}$$

where $\mathcal{A}$ is a constant matrix of dimension $m \times n$ and b is a vector in $\Re^m$. As described in the previous section, suppose that a fault-on trajectory is given and denoted as $x^f(t)$. Individual invariance theorem can be applied algorithmically in a power system transient stability by solving a feasibility problem to make sure that $\mathcal{P}$ is nonempty and then by substituting $x^f(t)$ in $\mathcal{P}$ to find the first instance at which $\{x^f(t)\} \bigcap \mathcal{P} = \emptyset$ as defined more explicitly in the following algorithm:

In the reduced model (13), each machine j can be used to construct an artificial system with a region of attraction A_i. With each artificial system i being invariant in its relevant set A_i, we can directly apply Corollary 1 on the original system (13) to prove that it remains invariant inside the intersection defined by $A_e = \bigcap_{i\in[1,m]} A_i$ as stated in the Corollary. Since

TABLE I
CCT ASSESSMENT RESULTS FOR THE 39-BUS SYSTEM (ASSOCIATED GRADIENT SYSTEM)

		Critical Clearing Time (CCT), s		
Faulted bus	Tripped line	Simulation	CUEP method	Proposed method
10	10-11	0.560	0.419	0.482
25	25-26	0.470	0.333	0.401
22	22-23	0.530	0.393	0.450
2	2-3	0.560	0.345	0.439
6	6-11	0.630	0.424	0.514

Algorithm 1 is used in this case for a polytopic estimation, let us denote $A_e = \mathcal{P}$ as the candidate region of attraction (polytope) and $x^f(t)$ as the fault-on trajectory which together with Δt, the simulation time step for the fault-on trajectory and, t_{max}, the maximum simulation time are inputs to the algorithm. In step 2, the algorithm starts by insuring that $\mathcal{P}$ is non-empty in order to proceed which can be checked easily by using interior point methods or linear solvers. Afterwards, the algorithm follows the fault-on trajectory inside $\mathcal{P}$ until either the fault-on trajectory escapes the estimated region of attraction $\mathcal{P}$ or reaches the maximum simulation time which would indicate the the fault-on trajectory lies entirely inside the estimated region. The algorithm terminates and reports the critical clearing time as $tc = 0$ if $\mathcal{P}$ was found to be empty, otherwise, a sequence of function evaluations is executed to maximize the critical clearing time t_c as in steps 8-10.

Generally, the shape and size of the estimated region of attraction will effect the estimated critical clearing time. We believe that a similar algorithm can be used with other types of estimations like ellipsoids, or convex hulls where the fault-on trajectory can be traced until it exits the estimated region in a similar fashion to what is described in Algorithm 1.

To test the proposed algorithm, A three phase fault is initiated at $t = 0$ in the locations given in Table I and is cleared by tripping the associated line. The fault-on trajectory is calculated by time domain simulation and fed to Algorithm 1 together with the region of attraction estimate A_e in order to find the time at which the fault-on trajectory exits the polytope A_e.

In this test, a controlling UEP approach was used to estimate CCT's in comparison to simulation-based assessment and the proposed method. By using the associated gradient system in (13), the Controlling UEP approach can be implemented as follows:

1) The first local maximum of the energy function (14) along the fault-on trajectory was determined at the point (δ^*) which denotes the exit point.
2) Using the exit point, δ^*, as an initial condition, the associated gradient system was integrated to find the controlling UEP, δ_{CO}.
3) The constant energy surface of (14) at δ_{CO} was used as a local approximation of the relative stability boundary.
4) The critical clearing time was determined as the time it takes the fault-on trajectory to meet the relative stability boundary found in step 3.

It can be seen from Table I that the algorithm succeeded in providing a very practical estimates of CCT. The maximum deviation occurred for a fault at bus 2 with 121 ms whereas

the minimum deviation was 69 ms for the contingency at bus 25. Similar to the previous case, we notice that the proposed approach provides less conservative CCT estimates in comparison to energy function approaches. It can be concluded from the results that the proposed method provided better estimates in all cases and that the CUEP method seemed to always provide more conservative estimate comparatively [16], [28].

B. New England 39-Bus System (Full-Order System)

The goal of this case study is to test the applicability of individual invariance in the full-order model (11) where methods like the BCU and PEBS can perform quiet well [16]. The model in (11) can be re-written as follows:

$$\begin{aligned}\dot{\delta}_i &= \omega_i \\ M_i\dot{\omega}_i &= P_i - \sum_{j=2}^{n} V_iV_jB_{i,j}\sin(\delta_{i,j}) \\ &\quad -V_iV_1B_{i,1}\sin(\delta_{i,1}) - D_i\omega_i \end{aligned} \tag{16}$$

Here we only separated the term $-V_iV_1B_{i,1}\sin(\delta_{i,1})$ together with the damping term to create an artificial system of the following form:

$$\begin{aligned}\dot{\delta}_i &= \omega_i \\ M_i\dot{\omega}_i &= -V_iV_1B_{i,1}\sin(\delta_{i,1}) - D_i\omega_i \end{aligned} \tag{17}$$

By removing the artificial system (17) from (16), we will be left with the coupling terms as in (13) which can be written as:

$$M_i\ddot{\delta}_i = P_i - \sum_{j=2}^{n} V_iV_jB_{i,j}\sin(\delta_{i,j}) \tag{18}$$

Similar to the previous section, (18) will be analyzed as an equivalent associated gradient system and we can find a polyhedron $\mathcal{P}$ defined by the inequality $|\delta_{i,j} - \delta^*_{i,j}| \leq \pi, \forall j \in [1, n]$ that is positively invariant for each machine i. In other words, A trajectory of (18) initiated inside $\mathcal{P}$ will remain in it for all future time. The analysis of artificial system (18) gives conditions on $|\delta_{i,j}|$ only and cannot produce conditions on ω_i but we can arrive at that from artificial system (17).

An auxiliary parameter α_i will be added to both vector fields while maintaining the original vector field (16) intact. The idea behind adding the auxiliary parameter is to tune the estimated region of attraction to be as large as possible.

$$\begin{aligned}M_i\ddot{\delta}_i &= P_i - \sum_{j=2}^{n} V_iV_jB_{ij}\sin(\delta_{i,j}) \\ &\quad -(1-\alpha_i)V_iV_1B_{i,1}\sin(\delta_{i,1}) \end{aligned} \tag{19}$$

$$\begin{aligned}\dot{\delta}_i &= \omega_i \\ M_i\dot{\omega}_i &= -\alpha_iV_iV_1B_{i1}\sin(\delta_{i,1}) - D_i\omega_i \end{aligned} \tag{20}$$

The right hand sides of (19) and (20) sum up to the same vector field of (16). With machine 1 as the slack bus, the reconstruction of (20) creates a classical system with a known energy function defined by:

$$V_i(\delta_{i,1}, \omega_i) = \frac{1}{2}M_i{\omega_i}^2 - \alpha_iV_iV_1B_{i,1}\cos(\delta_{i,1}) \tag{21}$$

$V_i(\delta_{i,1}, \omega_i)$ is an energy function for every system i in (20) and its derivative is $\frac{dV_i(\delta_{i,1},\omega_i)}{dt} \leq -D_i{\omega_i}^2$.

For each artificial system i in (20), a region of attraction can be defined as a sub-level set of the relevant energy function in (21), that is: $A_i = \{(\delta_{i,1}, \omega_i) \in \mathcal{P} : V_i(\delta_{i,1}, \omega_i) \leq C_i\}$, where C_i is defined as $C_i = V_i(\tilde{\delta}_{i,1}, 0)$ and $\tilde{\delta}_{i,1} \in \mathcal{P}$. In the 39-bus test system, 9 artificial systems of each form (19) and (20) will be used to assess its transient stability in Algorithm 2 as follows:

Algorithm 2

1. A polyhedron $\mathcal{P}$ is defined for (19) as the intersection of all the inequalities $|\delta_{i,j} - \delta^*_{i,j}| \leq \pi, \forall j \in [1, n]$ and $|\delta_{i,1}| \leq \pi, \forall i \in [1, n]$.
2. $V_i(\delta_{i,1}, \omega_i)$ is defined for each machine i in (20).
3. For each artificial system in (20), The constant energy surface of its respective energy function $V_i(\delta_{i,1}, \omega_i)$ is evaluated at $(\tilde{\delta}_{i,1}, 0)$ with $\tilde{\delta}_{i,1} \in \mathcal{P}$ to obtain the set A_i as an invariant set for the i^{th} artificial system.
4. The critical clearing time is determined as the maximum time at which no relative fault-on trajectory $(\delta_i(t)_{Fault-on}, \omega_i(t)_{Fault-on})$ exits the relative stability boundary found in step 3.

The construction of the artificial systems in this example ensures that the union of all the invariant sets A_i's will also be an invariant set for the original system since every set A_i is a subset of the polyhedron $\mathcal{P}$. The parameter α in (19) and (20) will affect the estimated region and needs to be carefully chosen, in our tests we set $\alpha_i = 1$ and $\alpha_i = \frac{1}{M_i}$.

Theorem I allowed us to reconstruct the vector field of the original system in a way that separates artificial machine states $(\delta_{i,1}, \omega_i)$ as given in (20) leading to an independent assessment of each machine's response to a disturbance. It also allowed us to separate the coupling parameters into an individual artificial system as in (19). In this section, the proposed approach was compared to a Controlling UEP method which is similar to the approach used previously except that a kinetic energy term in the form $\frac{1}{2}\omega^T M\omega$ is added to (14), the implementation closely follows the BCU methodology described in [16].

Table II demonstrates the results of three phase bus faults cleared by line tripping. For every fault, the Critical Clearing Time was estimated through exhaustive simulations, BCU, and the proposed method for two different artificial systems constructions one with $\alpha_i = 1$ and the other with $\alpha_i = \frac{1}{M_i}$. Clearly from the results the choice of $\alpha_i = 1$ provides poor estimation in comparison to the other methods, whereas, the choice of the larger $\alpha_i = \frac{1}{M_i}$ provided better estimates, this is associated with the fact that α_i increases the overall level-sets of its relevant energy function inside $\mathcal{P}$. In general, it compared favorably to the BCU approach in 5 out of 11 test cases for the full order model with an improved CCT estimates varying from a maximum of 0.0629 s to a minimum of 0.0096 s for faults at buses 25 and 22

TABLE II
CCT ASSESSMENT RESULTS FOR THE 39-BUS SYSTEM (FULL-ORDER SYSTEM)

		Critical Clearing Time (CCT), s			
Faulted bus	Tripped line	Simulation	BCU	$\alpha_i = 1$	$\alpha_i = \frac{1}{M_i}$
2	2-3	0.44	0.2831	0.240	0.317
5	5-8	0.52	0.3649	0.188	0.379
6	6-11	0.50	0.3510	0.187	0.367
10	10-11	0.46	0.3442	0.180	0.335
13	13-14	0.52	0.3970	0.186	0.357
16	16-24	0.50	0.3686	0.149	0.329
21	21-22	0.52	0.4377	0.154	0.325
22	22-23	0.42	0.3034	0.169	0.313
23	23-24	0.39	0.3172	0.141	0.290
25	25-26	0.36	0.2661	0.185	0.329
26	26-27	0.30	0.2844	0.169	0.281

respectively. On the other hand, the proposed method provided more conservative estimates in comparison to the BCU in 6 out of 11 test cases with CCT reduction varying from a maximum of 0.1127 s to a minimum of 0.0034 s for faults at buses 21 and 26 respectively. It should be noted that simulations in all cases considered the exact same model in (16), whereas in the previous section the simulations where on the reduced model (13) to maintain consistency in our comparisons. In addition to providing an adequate and fast assessment of CCT, Individual Invariance allows us to visualize the stability regions of each machine independently since the artificial systems are constructed to separate the internal angle and frequency of each machine in a 2-d system. This gives an insight into how the region of attraction is evolving with the change in system parameters and also indicates which machine is more stable or in the contrary more vulnerable to disturbances.

Figs. 7 and 8 depict the level sets of the energy functions associated with artificial systems 3 and 9 which reflects the speed-angle characteristics of machines 3 and 9 in the context of individual invariance after tripping the line 10-11 for $\alpha_i = 1$ and $\alpha_i = \frac{1}{M_i}$ respectively. For a fault at bus 10, the projected fault-on trajectory is depicted in each figure and it can be seen that the fault-on trajectory hits the boundary of $V_3 = C$ before reaching the boundary of $V_9 = C$. Hence, the CCT estimate of artificial system 3 will dictate the overall CCT assessment in this case given that all other boundaries for the remaining artificial systems are not breached. It is also clear that increasing α_i from 1 to $\frac{1}{M_i}$ has increased the energy levels and consequently enlarged the estimate allowing the fault-on trajectory to remain inside the region of attraction for a longer duration. Similarly, Figs. 9 and 10 depict the level sets of the energy functions associated with artificial systems 2 and 9 which reflect the speed-angle characteristics of machines 2 and 9 after tripping the line 5-8 for $\alpha_i = 1$ and $\alpha_i = \frac{1}{M_i}$ respectively. The same conclusion can be seen in this case except that machine 2 is more vulnerable in this test case instead of machine 3 which is valid since machine 2 (G31 in 6) is relatively closer to the faulted bus 5 whereas in the previous test, machine 3 (G32 in 6) is connected directly to the faulted bus 10 through a step-up transformer. In Figs. 11 and 12, we can see that our results are also proven by simulation with the system remaining transiently stable at the estimated CCT's. It is worth noting that in general, different energy functions may yield different results with respect to the BCU estimates. Also,

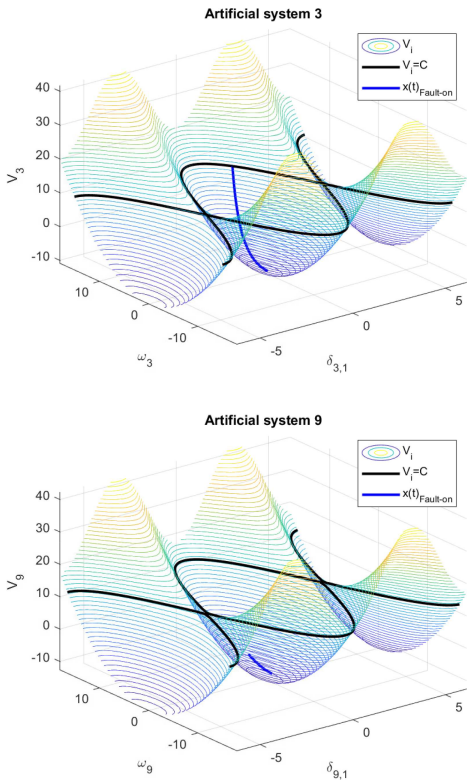

Fig. 7. Fault at bus 10, cleared at the estimated time of 0.335 s with $\alpha_i = \frac{1}{M_i}$.

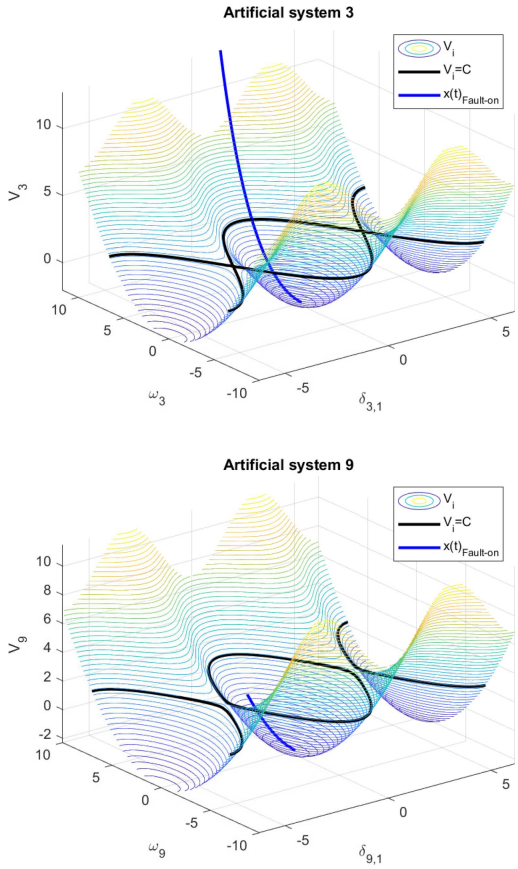

Fig. 8. Fault at bus 10, cleared at the estimated time of 0.335 s with $\alpha_i = 1$.

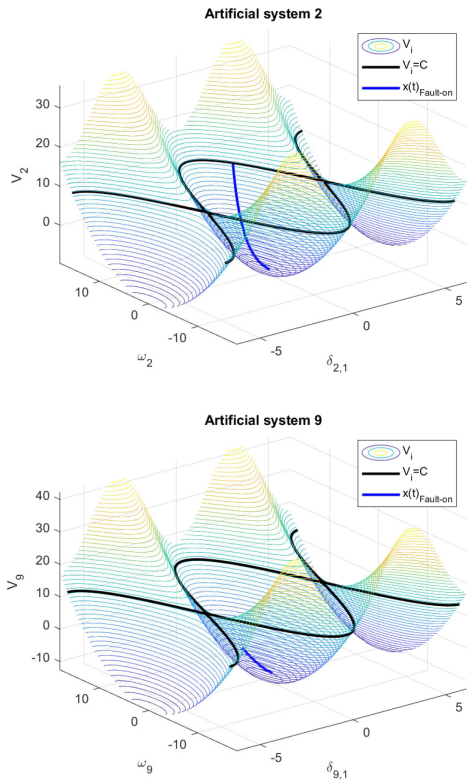

Fig. 9. Fault at bus 5, cleared at the estimated time of 0.379 s with $\alpha_i = \frac{1}{M_i}$.

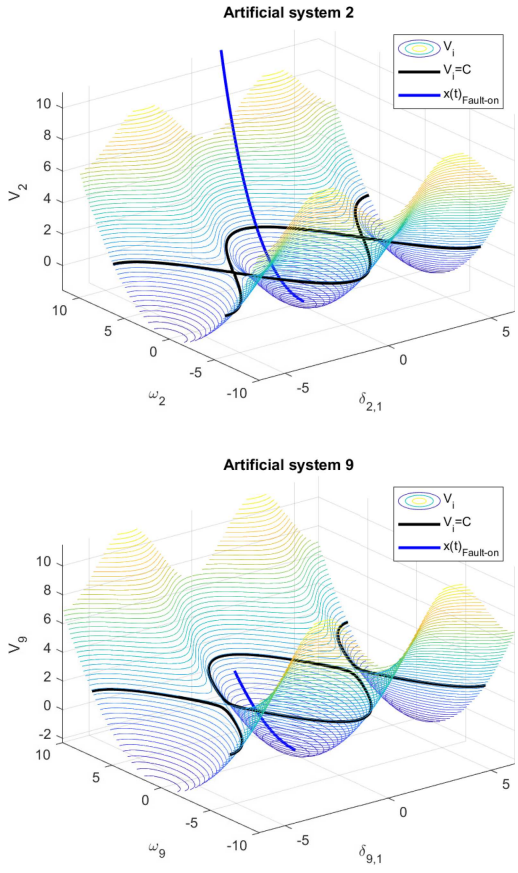

Fig. 10. Fault at bus 5, cleared at the estimated time of 0.379 s with $\alpha_i = 1$.

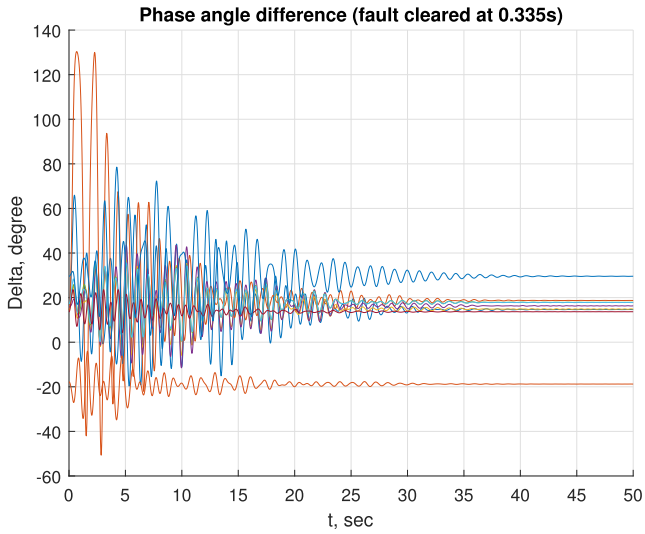

Fig. 11. Fault at bus 10, cleared at the estimated time of 0.335 s.

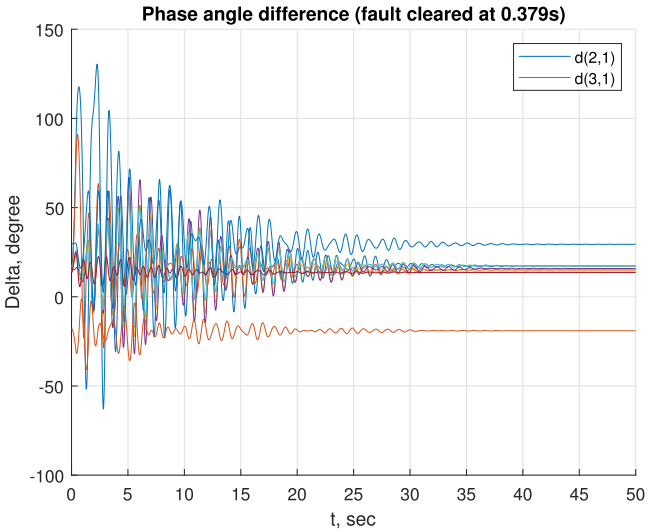

Fig. 12. Fault at bus 5, cleared at the estimated time of 0.379 s.

different artificial systems constructions and different auxiliary parameters can positively or negatively impact the estimates of an individual invariance-based approach. In this test, our main objective was to utilize the concept of individual invariance to separate the contribution of each machine's states toward maintaining or losing synchronism. This process gives more insight into what drives a power system into instability and what parameters need to be tuned or controlled to retain synchronism by individually assessing each artificial system.

VI. DC Microgrid With CPL

In this section, the stability of DC converter with Constant Power Loads will be studied. A DC converter connected to one

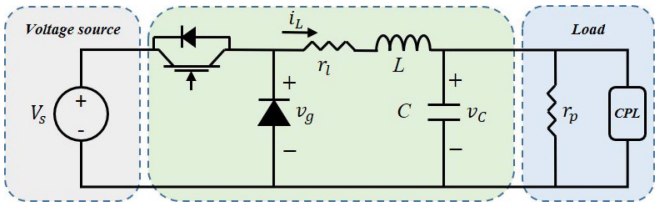

Fig. 13. DC converter with CPL.

CPL can be represented as follows:

$$\dot{x}_1 = -\frac{r_l}{L}x_1 - \frac{1}{C}x_2 + v_g$$
$$\dot{x}_2 = \frac{1}{L}x_1 - \frac{1}{r_pC}x_2 - CP\frac{1}{x_2} \tag{22}$$

The model is depicted in Fig. 13 and consists of a linear system, DC input (v_g), and a nonlinear term from the reciprocal of x_2 which arises from the constant power load. The individual invariance principle in Theorem 1 does not constrain our choice of individual vector fields, in this case we can choose the first artificial system as the linear part of (22) while the second artificial system will contain the rest of (22) as follows:

$$\dot{x} = f^1(x) = \begin{bmatrix} -\frac{r_l}{L}x_1 - \frac{1}{C}x_2 + v_g \\ -\frac{1}{2r_pC}x_2 \end{bmatrix}$$
$$\dot{x} = f^2(x) = \begin{bmatrix} 0 \\ \frac{1}{L}x_1 - \frac{1}{2r_pC}x_2 - CP\frac{1}{x_2} \end{bmatrix}$$

Note that the first system has an asymptotic stable equilibrium point since its state matrix A has real negative eigenvalues, so the whole state space is a region of attraction of that equilibrium point. One may conclude that the boundary of the stability region in (22) is then defined solely by the second artificial system but such conclusion is not necessarily true and great attention has to be paid in applying Theorem 1. The rational behind the structure of the second artificial system is to have all spatial variables of (22) present in one function only (in this case $\frac{dx_2}{dt}$) to force $f^2(x)$ to flow in x_2 direction and consequently defining an invariant set for that system will be easier.

This choice of $f^2(x)$ lead to a continuum of equilibrium points from the solution of the quadratic function:

$$f_2^2(x) = -\frac{1}{2r_pC}x_2^2 + \frac{1}{L}x_1x_2 - CP = 0$$

By solving the equation above, we will have two solutions at:

(a) $x_2 = \frac{r_pC}{L}x_1 + r_pC\sqrt{\frac{1}{L^2}x_1^2 - \frac{2P}{r_p}}, \quad \forall x_1 \geq L\sqrt{\frac{2P}{r_p}}$

(b) $x_2 = \frac{r_pC}{L}x_1 - r_pC\sqrt{\frac{1}{L^2}x_1^2 - \frac{2P}{r_p}}, \quad \forall x_1 \geq L\sqrt{\frac{2P}{r_p}}$

Analytically, we can determine that (a) is a stable continuum of equilibrium points and (b) is unstable by perturbing the system around the curve by some ϵ or by substitution in $f^2(x)$. We could also take advantage of the unidirectional flow of $f^2(x)$ and simulate one instance to evaluate the stability around both curves. The zero solution of $f_2^2(x)$ defines a smooth curve whose interior at $f_2^2(x) \geq 0$ is a convex set that is also positively invariant since all solutions within this set approach (a) as time goes to infinity. To better illustrate these results, we simulated both artificial systems as shown in Fig. 14. So far we developed a great understanding of the attractors in both artificial systems by mere algebraic analysis without the need of physics inspired methods like Energy or Lyapunov functions or exhaustive computer simulations. In fact, this approach is physically agnostic since neither artificial system represents a sound physical process independently rather each was constructed for the sole purpose of having an attainable invariant set. Those sets are defined as $A_1 = \{x \in \Re^2\}$ and $A_2 = \left\{x \in \Re^2 : x_2 \geq \frac{r_pC}{L}x_1 - r_pC\sqrt{\frac{1}{L^2}x_1^2 - \frac{2P}{r_p}}\right\}$.

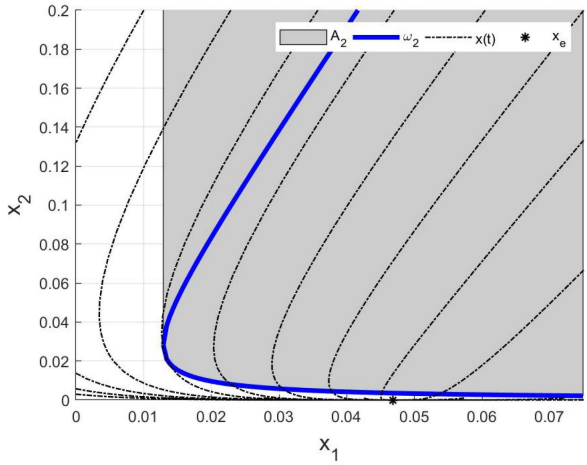

Fig. 14. Invariant sets of both artificial systems without auxiliary vector.

A_1 is basically the whole state space, while A_2 contains all solutions depicted in Fig. 14. With slight manipulation of those sets we will be able to satisfy Theorem 1 conditions. Theorem 1 requires all individual artificial systems to be stable in the same set A_e. In Fig. 14, we notice that the ω-limit of the first system (ω_1) lies outside the invariant set A_2. This can be fixed by introducing an auxiliary vector field $g(.)$ that shifts ω_1 to the interior of A_2. An auxiliary vector is a vector that appears in some or all artificial systems ($f^i(x)$) while remaining invisible to the original system $f(x)$. In this case, $g(.)$ is a constant vector of $[0, v_g]^T$ that is added to $f^1(x)$ and subtracted from $f^2(x)$.

$$\dot{x} = f^1(x) = \begin{bmatrix} -\frac{r_l}{L}x_1 - \frac{1}{C}x_2 + v_g \\ -\frac{1}{2r_pC}x_2 + \mathbf{v}_g \end{bmatrix} \tag{23}$$

$$\dot{x} = f^2(x) = \begin{bmatrix} 0 \\ \frac{1}{L}x_1 - \frac{1}{2r_pC}x_2 - CP\frac{1}{x_2} - \mathbf{v}_g \end{bmatrix} \tag{24}$$

With this alteration, we bring $\omega_1 \in A_2$ as shown in Fig. 15. Now we can take advantage of individual invariance by relying only on linear analysis to estimate the region of attraction of (23). In other words, studying the behavior of the linear system defined by $f^1(x)$ with respect to the previously defined regions. From the definition of A_1 and A_2, there intersection is A_2 thus it can serve as a candidate A_e in Theorem 1. To meet the criterion of Theorem 1, A_e needs to be positively invariant with respect to all individual systems and it is indeed for $f^2(x)$ which leaves us with the linear system $f^1(x)$ that has its equilibrium point inside A_2. By just a handful number of simulations of the individual

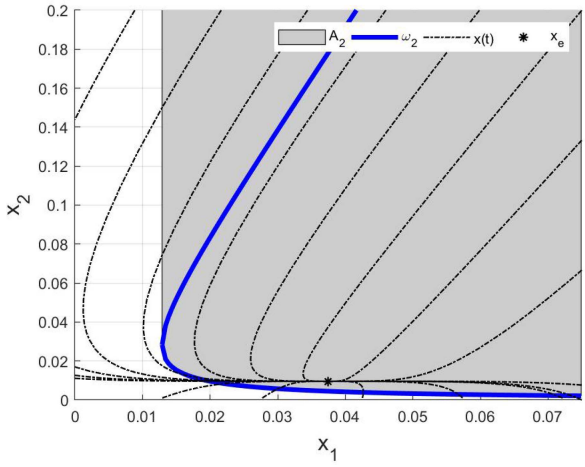

Fig. 15. Invariant sets of both artificial systems with auxiliary vector.

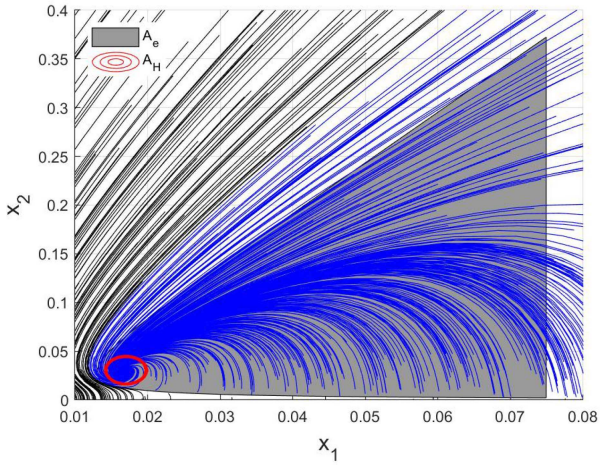

Fig. 16. Phase portrait of (22), A_e and A_H from [23].

linear system at the boundaries of A_2 we found that there exits a set $\hat{A}_e \subset A_2$ for which both systems are invariant, and we could quantify the following subset to be our estimated region of attraction:

$$A_e = \Big\{ x \in \Re^2 : x_1 \leq 0.075, \\ -\frac{1}{2r_p C} x_2^2 + \frac{1}{L} x_1 x_2 - CP + \mathbf{v}_g x_2 \geq 0 \Big\}$$

$$A_e \subset \hat{A}_e \subset A_2$$

This example proves that individual invariance can bring simplicity to problems deemed difficult and analytically intractable. In Fig. 16, it is clear that individual invariance provides significantly larger estimates of stability regions, the figure depicts the stability region estimate of the same system as given in [23] which is the ellipse A_H inside A_e (Shown also in close-up in Fig. 17). A_H estimation fades in comparison to our individual invariance based estimate as clearly seen in the figure where A_H only covers a very small region around the equilibrium point and the method in [23] lacks the generality of individual invariance and can only be applied to a type of port-Hamiltonian systems.

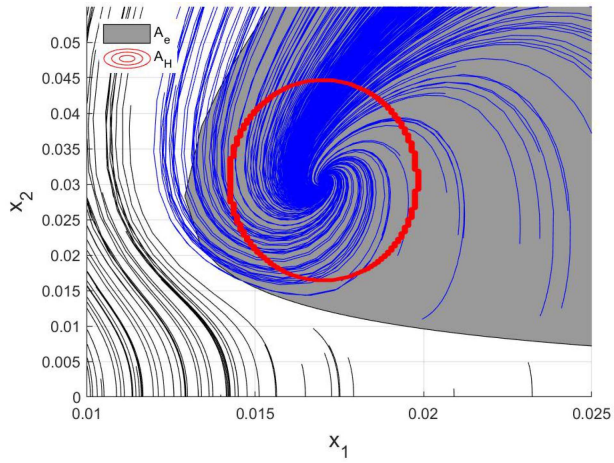

Fig. 17. Phase portrait of 22, A_e and A_H from [23].

VII. Future Perspectives

The Individual Invariance Theorem brings simplicity to the overly complex problem of stability in nonlinear systems by transforming the complicated nonlinear interactions into simpler lower dimensional artificial systems. This seemingly intuitive approach allows revisiting the question of regions of attraction from different angles, where the region of attraction approximation results from a decomposition of a given system into a set of artificial systems which allows altering and deforming the approximate by different choices of artificial systems. This two-step approach, identifying artificial systems then approximating the region of attraction, provides an insight into what elements of a given vector field are participating in the shape and size of the region of attraction. Although in this article, we presented several successful implementations of the Theorem, there are key areas to be explored. For instance, an artificial system can be used to characterize an uncertain parameter (or disturbance) to independently evaluate its impact on the overall system stability without the need to simulate the whole model. Similarly, control parameters can be designed and tuned as artificial systems interacting with the model. These are some general implications that are currently under development. In power systems, individual invariance can provide an insightful look into what drives the system toward instability by independently assessing each artificial system which can be a power plant or a single generator. The next step to applying individual invariance for stability assessment in power systems will be to evaluate different artificial system constructions and evaluate the evolution of regions of attraction with each artificial system. Similar to energy functions, defining artificial systems will depend on the system physics, however, the flexibility margin is significantly higher and we believe that this concept provides a new perspective to the problem of stability that is capable of overcoming some limitations of classical methods.

VIII. Conclusion

This article presents a novel approach for estimating the region of attraction in nonlinear autonomous systems based on

new theoretical findings. A nonlinear vector field is represented as a sum of individual vector fields of the same dimension. Each individual vector field creates an artificial system where its region of attraction is defined independently of the original system. The individual invariance Theorem states that if all individual vector fields are invariant in the same set then that set is invariant for the original system. This article provides the theoretical foundation of this novel result and extends it to an algorithmic construction of regions of attraction. The presented theory is introduced through several second order examples followed by more practical and high order test cases in power systems including reduced-order and full-order models and a DC application with nonlinear loads. A major advantage of individual invariance theorem is that it allows the use of linear programs to approximate subsets of the region of attraction as an intersection of polyhedrons which provide a computationally efficient approach for transient stability studies in power system. It also allows for analytical description of subsets of the region of attraction as used in the estimates of the 39-bus full-order model which can be of significant value in real-world applications. However, we expect the current implementation to provide slightly conservative assessment of stability in larger power systems in comparison to direct methods for two reasons: 1- Direct methods provide stability assessment relevant to each fault-on trajectory, whereas, individual invariance provide a system based assessment, 2- The bounds on the coupling terms eliminate some stable cases where a power system can experience large deviations while retaining stability. This is only true in the context of CCT assessment, otherwise, we consider the individual invariance as a qualitative analysis tool that is capable of providing critical insight into nonlinear systems behavior.

APPENDIX A
TEST SYSTEMS' PARAMETERS

New England 39-bus system [15]			
Parameter	Value	Parameter	Value
H_1	42.0 s	x'_{d1}	0.0310 pu
H_2	30.2 s	x'_{d2}	0.0697 pu
H_3	35.8 s	x'_{d3}	0.0531 pu
H_4	28.6 s	x'_{d4}	0.0436 pu
H_5	26.0 s	x'_{d5}	0.0660 pu
H_6	34.8 s	x'_{d6}	0.0500 pu
H_7	26.4 s	x'_{d7}	0.0490 pu
H_8	24.3 s	x'_{d8}	0.0570 pu
H_9	34.5 s	x'_{d9}	0.0570 pu
H_{10}	31.0 s	x'_{d10}	0.0457 pu

Parameters of DC converter with CPL [23]					
C	P	L	v_g	r_l	r_p
2 mF	1 kW	78 μH	24 V	0.04 Ω	0.1 Ω

REFERENCES

[1] H. K. Khalil, *Nonlinear Systems*, vol. 2, no. 5. Hoboken, NJ, USA: Prentice-Hall, 1996.

[2] D. J. Hill and C. N. Chong, "Lyapunov functions of Lur'e-postnikov form for structure preserving models of power systems," *Automatica*, vol. 25, no. 3, pp. 453–460, 1989.

[3] R. Genesio, M. Tartaglia, and A. Vicino, "On the estimation of asymptotic stability regions: State of the art and new proposals," *IEEE Trans. Autom. Control*, vol. 30, no. 8, pp. 747–755, Aug. 1985.

[4] L. Vandenberghe and S. Boyd, "Semidefinite programming," *SIAM Rev.*, vol. 38, no. 1, pp. 49–95, 1996.

[5] S. Boyd, L. El Ghaoui, E. Feron, and V. Balakrishnan, *Linear Matrix Inequalities in System and Control Theory*. Philadelphia, PA, USA: Soc. Ind. Appl. Math., 1994.

[6] P. A. Parrilo, "Structured semidefinite programs and semialgebraic geometry methods in robustness and optimization," Ph.D. dissertation, California Inst. Technol., Pasadena, CA, USA, 2000.

[7] T. L. Vu and K. Turitsyn, "Lyapunov functions family approach to transient stability assessment," *IEEE Trans. Power Syst.*, vol. 31, no. 2, pp. 1269–1277, Mar. 2016.

[8] A. A. Ahmadi and P. A. Parrilo, "Non-monotonic Lyapunov functions for stability of discrete time nonlinear and switched systems," in *Proc. 47th IEEE Conf. Decis. Control*, 2008, pp. 614–621.

[9] R. Bellman, "Vector Lyanpunov functions," *J. Soc. Ind. Appl. Math., Ser. A: Control*, vol. 1, no. 1, pp. 32–34, 1962.

[10] W. M. Haddad and V. Chellaboina, *Nonlinear Dynamical Systems and Control: A Lyapunov-Based Approach*. Princeton, NJ, USA: Princeton Univ. Press, 2008.

[11] S. G. Nersesov and W. M. Haddad, "On the stability and control of nonlinear dynamical systems via vector Lyapunov functions," *IEEE Trans. Autom. Control*, vol. 51, no. 2, pp. 203–215, Feb. 2006.

[12] S. G. Nersesov, W. M. Haddad, and Q. Hui, "Finite-time stabilization of nonlinear dynamical systems via control vector Lyapunov functions," *J. Franklin Inst.*, vol. 345, no. 7, pp. 819–837, 2008.

[13] F. Prabhakara, A. El-Abiad, and A. Koivo, "Application of generalized Zubov's method to power system stability," *Int. J. Control*, vol. 20, no. 2, pp. 203–212, 1974.

[14] H.-D. Chang, C.-C. Chu, and G. Cauley, "Direct stability analysis of electric power systems using energy functions: Theory, applications, and perspective," *Proc. IEEE*, vol. 83, no. 11, pp. 1497–1529, Nov. 1995.

[15] A. Pai, *Energy Function Analysis for Power System Stability*. Berlin, Germany: Springer, 2012.

[16] ong Chiang, F. F. Wu, and P. P. Varaiya, "A BCU method for direct analysis of power system transient stability," *IEEE Trans. Power Syst.*, vol. 9, no. 3, pp. 1194–1208, Aug. 1994.

[17] M. Anghel, F. Milano, and A. Papachristodoulou, "Algorithmic construction of Lyapunov functions for power system stability analysis," *IEEE Trans. Circuits Syst. I, Reg. Papers*, vol. 60, no. 9, pp. 2533–2546, Sep. 2013.

[18] G. Chesi, *Domain of Attraction: Analysis and Control Via SOS Programming*, vol. 415. Berlin, Germany: Springer, 2011.

[19] C. Zhang, M. Molinas, Z. Li, and X. Cai, "Synchronizing stability analysis and region of attraction estimation of grid-feeding VSCs using sum-of-squares programming," *Front. Energy Res.*, vol. 8, 2020.

[20] M. Z. Mansour, S. P. Me, S. Hadavi, B. Badrazadeh, A. Karimi, and B. Bahrani, "Nonlinear transient stability analysis of phase-locked loop based grid-following voltage source converters using Lyapunov's direct method," *IEEE J. Emerg. Sel. Topics Power Electron.*, vol. 10, no. 3, pp. 2699–2709, Jun. 2022.

[21] Z. Zhang, R. Schuerhuber, L. Fickert, F. Katrin, C. Guochu, and Z. Yongming, "Domain of Attraction's estimation for grid connected converters with phase-locked loop," *IEEE Trans. Power Syst.*, vol. 37, no. 2, pp. 1351–1362, Mar. 2022.

[22] A. Emadi, A. Khaligh, C. H. Rivetta, and G. A. Williamson, "Constant power loads and negative impedance instability in automotive systems: Definition, modeling, stability, and control of power electronic converters and motor drives," *IEEE Trans. Veh. Technol.*, vol. 55, no. 4, pp. 1112–1125, Jul. 2006.

[23] P. Monshizadeh, J. E. Machado, R. Ortega, and A. van der Schaft, "Power-controlled hamiltonian systems: Application to electrical systems with constant power loads," *Automatica*, vol. 109, 2019, Art. no. 108527.

[24] S. M. Al Araifi, M. S. E. Moursi, and S. M. Djouadi, "Individual functions method for power system transient stability assessment," *IEEE Trans. Power Syst.*, vol. 35, no. 2, pp. 1264–1273, Mar. 2020.

[25] F. Blanchini, "Set invariance in control," *Automatica*, vol. 35, no. 11, pp. 1747–1767, 1999.

[26] J.-P. Aubin, *Viability Theory*. Boston, MA, USA: Birkhauser Boston Inc., 1991.

[27] R. M. Redheffer, "The theorems of bony and brezis on flow-invariant sets," *Amer. Math. Monthly*, vol. 79, no. 7, pp. 740–747, 1972. [Online]. Available: http://www.jstor.org/stable/2316263
[28] H.-D. Chiang, *Direct Methods for Stability Analysis of Electric Power Systems*. New York, NY, USA: Wiley, 2010.
[29] H.-D. Chiang and L. F. Alberto, *Stability Regions of Nonlinear Dynamical Systems: Theory, Estimation, and Applications*. Cambridge, U.K.: Cambridge Univ. Press, 2015.
[30] P. Kundur et al., "Definition and classification of power system stability IEEE/CIGRE joint task force on stability terms and definitions," *IEEE Trans. Power Syst.*, vol. 19, no. 3, pp. 1387–1401, Aug. 2004.
[31] N. G. Bretas and L. F. C. Alberto, "Lyapunov function for power systems with transfer conductances: Extension of the invariance principle," *IEEE Trans. Power Syst.*, vol. 18, no. 2, pp. 769–777, May 2003.

Surour Alaraifi received the B.Sc. degree in electrical engineering from the United Arab Emirates University, Alain, UAE, in 2010, the M.Sc. and Ph.D. degrees in electrical engineering from the Masdar Institute of Science and Technology, Khalifa University, Abu Dhabi, UAE, in 2013 and 2018. He worked with Transco, Abu Dhabi, as a Senior Planning Engineer. He was with Emirates Water and Electricity company (EWEC), Abu Dhabi, as a senior network studies engineer. He is currently a Postdoctoral Fellow with the Electrical Engineering and Computer Science Department, Khalifa University, Abu Dhabi. He is also currently a visiting Scientist with the School of Electrical and Computer Engineering at Cornell University, Ithaca, NY, USA. His research interests include power system stability, dynamics of renewable energy systems, and numerical methods for large scale nonlinear networks.

Seddik Djouadi (Senior Member, IEEE) received the B.S. degree (Hons.) in electrical engineering from the Ecole Nationale Polytechnique, El Harrach, Algeria, the M.Sc. degree in electrical engineering from the University of Montreal, Montreal, QC, Canada, and the Ph.D. degree from McGill University, Montreal. He is currently a Full Professor with the Electrical Engineering and Computer Science Department, The University of Tennessee, Knoxville, TN, USA. He has authored or coauthored more than about hundred journal and conference papers, some of which were invited papers. His research interests include filtering and control of systems under communication constraints, modeling and control of wireless networks, control systems and applications to autonomous sensor platforms, electromechanical and mobile communication systems, in particular smart grid and power systems, control systems through communication links, networked control systems, and model reduction for aerodynamic feedback flow control. He was the recipient of the best PES paper award in 2022, American Control Conference Best Student Paper Certificate (best five in competition), in 1998, Tibbet Award from AFS Inc., in 1999, Ralph E. Powe Junior Faculty Enhancement Award, in 2005, and Best Paper Award at the 1st Conference on Intelligent Systems and Automation, in 2008.

Mohamed Shawky El Moursi (Senior Member, IEEE) received the B.Sc. and M.Sc. degrees in electrical engineering from Mansoura University, Mansoura, Egypt, in 1997 and 2002, respectively, and the Ph.D. degree in electrical engineering from the University of New Brunswick (UNB), Fredericton, NB, Canada, in 2005. From 2002 to 2005, he was a Research and Teaching Assistant with the Department of Electrical and Computer Engineering, UNB. He joined McGill University as a Postdoctoral Fellow with the Power Electronics Group. He was with Vestas Wind Systems, Arhus, Denmark, in the Technology R&D with the Wind Power Plant Group. He was with TRANSCO, UAE, as a Senior Study and Planning Engineer. He is currently a Professor with the Electrical Engineering and Computer Science Department and the Deputy Director of Advanced Power and Energy Center (APEC), Khalifa University, Abu Dhabi, UAE, and seconded to a distinguished Professor position with the Faculty of Engineering, Mansoura University, Mansoura, Egypt and currently on leave. He was a Visiting Professor with the Massachusetts Institute of Technology, Cambridge, Massachusetts, USA. His research interests include renewable energy systems (Wind and PV) integration, power system, FACTS technologies, VSC-HVDC systems, Microgrid operation and control and AI applications in power systems. Dr. Shawky El Moursi is currently the Editor of IEEE TRANSACTIONS ON POWER DELIVERY, IEEE TRANSACTIONS ON POWER SYSTEMS, an Associate Editor for IEEE TRANSACTIONS ON POWER ELECTRONICS, and IEEE TRANSACTIONS ON SMART GRID, the Guest Editor of IEEE TRANSACTIONS ON ENERGY CONVERSION, Guest Editor-in-Chief for special section between TPWRD and TPWRS, the Editor of IEEE Power Engineering Letters, Regional Editor for *IET Renewable Power Generation* and Associate Editor for *IET Power Electronics Journals*.